

Temperature and *Para*-Substituent Effects on the Face Selectivity of 1,3-Dipolar Cycloaddition Reactions of Benzonitrile Oxides with 5-Substituted Adamantane-2-thiones, *N*-Benzyladamantyl-2-imines, and 2-Methyleneadamantanes

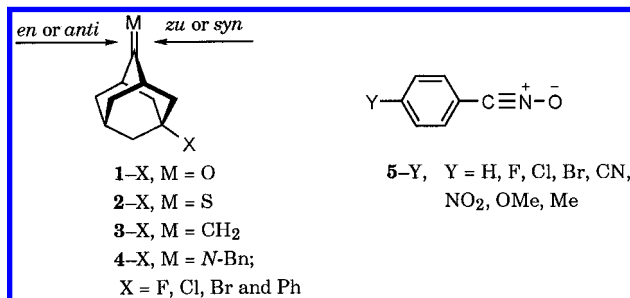
Tzong-Liang Tsai,[†] Wei-Cheng Chen,[‡] Chin-Hui Yu,[‡] W. J. le Noble,[§] and Wen-Sheng Chung^{*,†}

Department of Applied Chemistry, National Chiao Tung University, Hsinchu, Taiwan 30050, Republic of China; Department of Chemistry, National Tsing Hua University, Hsinchu, Taiwan 300, Republic of China; and Department of Chemistry, State University of New York, Stony Brook, New York 11794

Received May 19, 1998

The 1,3-dipolar cycloaddition reactions of *para*-substituted benzonitrile oxides (**5-Y**) with 5-fluoroadamantane-2-thione (**2-F**) and -2-methyleneadamantane (**3-F**) as well as with variously 5-substituted-*N*-benzyladamantyl-2-imines (**4-X**) were examined. They produce two geometrically isomeric Δ^2 -1,4,2-oxathiazolines (**7-F,Y**), Δ^2 -isoxazolines (**8-F,Y**), and Δ^2 -1,2,4-oxadiazolines (**11-X,Y**), respectively. The face selectivity in the latter reaction was found to be ~1:1 regardless of the variations in 5-substituent and the temperature. For the former two reactions, the *para*-substituent was varied from electron-withdrawing ($Y = F, Cl, Br, CN$, or NO_2) to -releasing ($Y = Me$, or OMe). The face selectivity was measured in all cases. The differences $\Delta\rho$ for the reactions of **2**- and **3-F** with **5-Y** were obtained from linear Hammett plots; they are +0.12 and 0.0, respectively. These low values and information from previous studies imply a concerted one-step mechanism with very little charge distribution differences in the transition states. These effects of temperature on the *Z/E* product ratios provide us, for the first time, with activation parameter differences between the *syn*- and *anti* transition states; their values are discussed. The product bias resulting from the favored attack of nitrile oxide on the *zu* face is discussed in terms of transition state hyperconjugation based on the experimental results and AM1 calculations.

The study of electronic effects in various sterically unbiased trigonal carbon centers continues to attract considerable theoretical and experimental attention.^{1,2} Among the many models, transition-state hyperconjugation^{1a–c,2} and electrostatic field interaction^{1c–e} are the two most popular explanations for the face selectivity results to be found in the literature. 5-Substituted adamantan-2-ones **1-X** and their derivatives have proven to be useful probes in research aimed at understanding the electronic factors in face selection.^{1a} These studies of a variety of reactions indicate that the reagent prefers to attack the face antiperiplanar to the more electron-rich vicinal bonds (*zu* and *en* face preference in **1-X** when *X* equals an electron-withdrawing or -donating group, respectively). These results can be reconciled with Cieplak's transition-state hyperconjugation model.² That interpretation allows but does not demand that the magnitude of the effect may be a function of the electronic nature of the nucleophile or electrophile. There is only



one example of a search for such an effect: in the addition of *para*-substituted phenyl Grignard reagents to **1-F**, the substituent was varied from CF_3 to NMe_2 .³ However, no effect was found on the face selectivity.

1,3-Dipolar cycloadditions offer a convenient one-step route for the construction of a variety of complex five-membered heterocycles which are synthetically useful compounds.⁴ Nitrile oxide cycloadditions to terminal alkenes and thiones proceed regioselectively to give 5-substituted Δ^2 -isoxazolines and Δ^2 -1,4,2-oxathiazolines, respectively.⁵ We recently reported⁶ the 1,3-dipolar cy-

(3) Lin, M.-H.; Silver, J. E.; le Noble, W. J. *J. Org. Chem.* **1988**, *53*, 5155.

(4) For reviews, see (a) Huisgen, R. In *1,3-Dipolar Cycloaddition Chemistry*; Padwa, A., Ed.; Wiley: New York, 1984; Vol. 1, pp 1–176. (b) Caramella, P.; Grünanger, P. In *1,3-Dipolar Cycloaddition Chemistry*; Padwa, A., Ed.; Wiley: New York, 1984; Vol. 1, pp 291–392. (c) *Nitrile Oxides, Nitrones, and Nitronates in Organic Synthesis*; Torsell, K. B. G., Ed.; VCH: New York, 1988. (d) Carruthers, W. *Cycloaddition Reactions in Organic Synthesis*; Pergamon Press: Oxford, 1990; pp 269–367. (e) Houk, K. N.; Gonzalez, J.; Li, Y. *Acc. Chem. Res.* **1995**, *28*, 81. (f) Sustmann, R. *Tetrahedron Lett.* **1971**, *2717*, 2721.

[†] National Chiao Tung University.

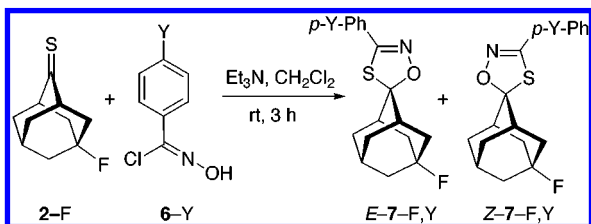
[‡] National Tsing Hua University.

[§] State University of New York.

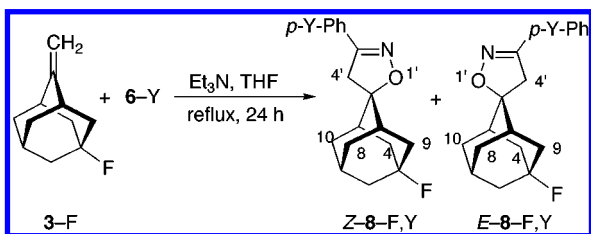
(1) (a) Bodepudi, V. R.; le Noble, W. J. *J. Org. Chem.* **1994**, *59*, 3265; **1991**, *56*, 2001 and references therein. (b) Halterman, R. L.; McCarthy, B. A.; McEvoy, M. A. *J. Org. Chem.* **1992**, *57*, 5585 and references therein. (c) For an excellent article on the electrostatic vs hyperconjugation effects, see Adcock, W.; Cotton, J.; Trout, N. A. *J. Org. Chem.* **1994**, *59*, 1867 and references therein. (d) Coxon, J. M.; Houk, K. N.; Luibrand, R. T. *J. Org. Chem.* **1995**, *60*, 418. (e) Paddon-Row, M. N.; Wu, Y.-D.; Houk, K. N. *J. Am. Chem. Soc.* **1992**, *114*, 10638 and references therein.

(2) (a) Cieplak, A. S.; Tait, B. D.; Johnson, C. R. *J. Am. Chem. Soc.* **1989**, *111*, 8447. (b) Cieplak, A. S. *J. Am. Chem. Soc.* **1981**, *103*, 4540. (c) Johnson, C. R.; Tait, B.; Cieplak, A. S. *J. Am. Chem. Soc.* **1987**, *109*, 5875.

Scheme 1



Scheme 2



cloaddition reactions of benzonitrile oxide (**5-H**) with the sterically unbiased thiones **2-X** and terminal alkenes **3-X** (where X = F, Cl, Br, and Ph) and found that the favored products derive from attack of nitrile oxide on the *zu*-face. Thus, 1,3-dipolar cycloaddition reactions to **2** and **3** provide additional important support for the transition-state hyperconjugation model, which stresses that the newly developing σ^* orbital of an incipient bond should attract electron density with the same directional preference, regardless of the type of reaction.^{1a,2c}

Several important questions remained to be answered: (1) Is there any effect of the *para*-substituent of phenyl nitrile oxide in these reactions, and can one obtain charge distribution information from the Hammett plot studies? (2) Are the reaction rates and the *E/Z* product ratios of 1,3-dipolar cycloadditions sensitive to the reaction temperature, and can one obtain activation parameter differences of the two transition states? (3) How do the HOMO and LUMO energies of the dipolarophiles (**1-X** to **4-X**) and dipoles (**5-Y**) vary with the substituents? With these objectives in mind, we synthesized a series of *para*-substituted benzonitrile oxides (**5-Y**) and studied the face selectivity of their reactions with **2-F** and **3-F**. The results from theoretical calculations (AM1) were compared with experimental results. The activation parameter differences and the difference in $\Delta\rho$ between the two 1,3-dipolar cycloaddition reactions supplement those previously given⁶ and allow us to comment on the mechanism.

Results and Discussion

The 1,3-dipolar cycloaddition reactions of **2-X** and **3-X** with parent nitrile oxide **5-H** in methylene chloride at room temperature give mixtures of *E*- and *Z*-adducts of **7-X,H** and **8-X,H** in 75–82% yields (Schemes 1 and 2).⁶ Compounds **2-F** and **3-F** were chosen for further study with *para*-substituted benzonitrile oxides **5-Y** (prepared *in situ* from the reaction of **6-Y** with triethylamine); the fluorine-induced chemical shifts and C-F couplings allow

Table 1. 1,3-Dipolar Cycloaddition Reaction of *Para*-Substituted Benzonitrile Oxide (**5-Y**) with 5-Fluoroadamantane-2-thiones (**2-F**) in Methylene Chloride at Room Temperature for 3 h

entry	σ_p^a	Y	<i>E</i> : <i>Z</i> - 7-F,Y ^b	yield, %
1	0	H	69:31	82
2	0.78	NO ₂	c	88
3	0.66	CN	71:29	89
4	0.06	F	68:32	85
5	0.23	Cl	68:32	94
6	0.23	Br	68:32	78
7	-0.17	CH ₃	66:34	80
8	-0.27	OCH ₃	65:35	86

^a The σ_p values are obtained from Swain, C. G.; Lupton, E. C., Jr. *J. Am. Chem. Soc.* **1968**, *90*, 4328. ^b The ratios of the adducts were determined by VPC analysis. ^c Ratio could not be determined by this method.

Table 2. 1,3-Dipolar Cycloaddition Reaction of *Para*-Substituted Benzonitrile Oxide (**5-Y**) with 5-Fluoro-2-Methyleneadamantanes (**3-F**) in Refluxing Tetrahydrofuran for 24 h

entry	σ_p	Y	<i>Z</i> : <i>E</i> - 8-F,Y ^a	yield, %
1	0.00	H	60:40	72
2	0.78	NO ₂	61:39	88
3	0.66	CN	60:40	83
4	0.06	F	59:41	85
5	0.23	Cl	61:39	79
6	0.23	Br	60:40	82
7	-0.17	CH ₃	60:40	77
8	-0.27	OCH ₃	59:41	81

^a The ratios of the *E*- and *Z*-adducts were determined by ¹H-NMR.

a straightforward assignment of configuration of the two products. Both adducts are stable to the reaction conditions, and they are characterized as 5-fluoro-3'-*p*-Y-phenyladamantane-2-spiro-5'-(Δ^2 -1',4',2'-oxathiazolines) based on their mass and NMR spectra.⁶ In all instances examined (Y = NO₂, CN, F, Cl, Br, OMe, and Me) the yields of *E*- and *Z*-**7-F,Y** are 78–94%, and the major isomer is *E*-**7-F,Y**, which results from syn attack of the nitrile oxide (**5-Y**) on **2-F** (see Table 1).

The configuration assignment of the epimers **7-F,Y** was based on the relative shielding power of oxygen vs sulfur directly “above” the flanking methylene groups. Thus, C-4 and C-9 (identified by their ¹⁹F coupling) are syn to the oxygen since they are shielded vs C-8 and C-10 by a margin of ≥ 2.2 ppm. The configurations of *Z*-**7-F,H** and *Z*-**7-Br,H** were established independently by means of both X-ray diffraction and a ¹³C NMR additivity scheme.^{6,8} The ¹³C NMR absorption peaks for the adamantane skeleton in the oxathiazolines *E*- and *Z*-**7-F,Y** are very similar to those observed for parent compounds *E*- and *Z*-**7-F,H**. Thus, the assignment of configuration is straightforward, based on these ¹³C NMR peaks (see Experimental Section).

The reactions of benzonitrile oxides **5-Y** with **3-F** were carried out in refluxing THF for 24 h to give two isoxazolines **8-F,Y** in 72–88% isolated yields (see Scheme 2 and Table 2). Again, the products were proven to be stable under the reaction conditions; i.e., both products are formed in kinetically controlled processes. In all

(5) (a) Huisgen, R.; Fisera, L.; Giera, H.; Sustmann, R. *J. Am. Chem. Soc.* **1995**, *117*, 9671. (b) Sustmann, R.; Sicking, W.; Huisgen, R. *ibid.* **1995**, *117*, 9679. (c) Fisera, L.; Huisgen, R.; Kalwinski, I.; Langhals, E.; Li, X.; Mloston, G.; Polborn, K.; Rapp, J.; Sicking, W.; Sustmann, R. *Pure Appl. Chem.* **1996**, *68*, 789. (d) Metzner, P. *Pure Appl. Chem.* **1996**, *68*, 863. (e) Grundmann, C. *Synthesis* **1970**, 344.

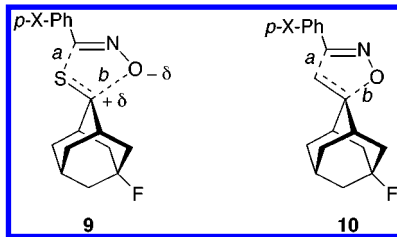
(6) Chung, W.-S.; Tsai, T.-L.; Ho, C.-C.; Chiang, M. Y. N.; le Noble, W. J. *J. Org. Chem.* **1997**, *62*, 4672.

(7) (a) Chung, W.-S.; Turro, N. J.; Srivastava, S.; Li, H.; le Noble, W. J. *J. Am. Chem. Soc.* **1988**, *110*, 7882. (b) Katada, T.; Eguchi, S.; Sasada, T. *J. Org. Chem.* **1986**, *51*, 314. (c) Li, H.; Silver, J. E.; Watson, W. H.; Kashyap, R. P.; le Noble, W. J. *J. Org. Chem.* **1991**, *56*, 5932.

(8) Srivastava, S.; Cheung, C.-K.; le Noble, W. J. *Magn. Reson. Chem.* **1985**, *23*, 232.

instances examined, the major isomer (\sim 60:40 ratio as determined by ^1H NMR integration) has the *Z* configuration. It should be noted that the major product **Z-8-F,Y** is derived from *syn* attack of the nitrile oxide on **3-F**. A 5.8% NOE was observed for the flanking pair axial-hydrogens at C-8 and C-10 but not at C-4 and C-9 when the 4'-methylene hydrogens were irradiated, confirming the major isomer to be **Z-8-F,Y**.

The data in Tables 1 and 2 show the previously noted tendency that all dipoles (**5-Y**) prefer to approach from the direction antiperiplanar to the electron richest bonds. In the Hammett plots of $\log(\text{syn/anti})$ vs σ_p , linear correlation are found; they give the reaction constant difference $\Delta\rho$ as 0.12 for **2-F** and 0.0 for **3-F**. These small values are accommodated by a one-step concerted mechanism involving a five-membered dipolar transition state **9**. This mechanism is consistent with previous experimental data, namely the low sensitivity of the rate constants to solvent polarity.⁶ A charge imbalance in the transition state has been suggested⁹ to explain the substituent and solvent effects of other concerted 1,3-dipolar cycloadditions. The values of $\Delta\rho$ also indicate that the dipole (CNO group) is acting as an electron acceptor and the dipolarophile (C=S or C=C) as an electron donor; the formation of partial charges in the transition states **9** and **10** suggests that bonds *a* in **9** and **10** have developed further than bonds *b*. However, this varies somewhat with the polar nature of the dipolarophiles, as indicated by the $\Delta\rho$ values.⁹ The fact that the $\Delta\rho$ value



in **3-F** is smaller than that in **2-F** points to a lowering of the polarity of the transition state **10**. Recent ab initio calculations by Huisgen and Sustmann^{5a-c} for the parent nitrone with dipolarophiles C=S vs C=C also support different transition states in these 1,3-dipolar cycloaddition reactions.

Some 1,3-dipolar cycloaddition reactions are controlled mainly by the HOMO (dipole)–LUMO (dipolarophile) interaction and others by the LUMO (dipole)–HOMO (dipolarophile) interaction. The smaller the energy gap between the controlling orbitals is, the faster is the reaction.^{4,5} The former is accelerated by electron-donating substituents in the dipole and electron-attracting substituents in the dipolarophile, and the latter by electron-donating substituents in the dipolarophile; in each case, the energy gap between the controlling orbitals in the two components is diminished. AM1 calculations of the HOMO–LUMO energy of **1-H** to **4-H** (Figure 1) reveal that all of the 1,3-dipolar reactions described here fit into the latter category; i.e., the nitrile oxide has a low lying LUMO which interacts with the HOMO of the dipolarophiles (**1-X** to **4-X**).

(9) (a) Dondoni, A.; Barbaro, G. *J. Chem. Soc., Perkin Trans. 2*, **1973**, 1769. (b) Ito, K.; Saito, K.; Takahashi, K. *Heterocycles* **1993**, **36**, 21. (c) Ito, K.; Saito, K. *Bull. Chem. Soc. Jpn.* **1995**, **68**, 3539. (d) Balsamini, C.; Bedini, A.; Spadoni, G.; Burdisso, M.; Capelli, A. M. *Tetrahedron* **1994**, **50**, 3773.

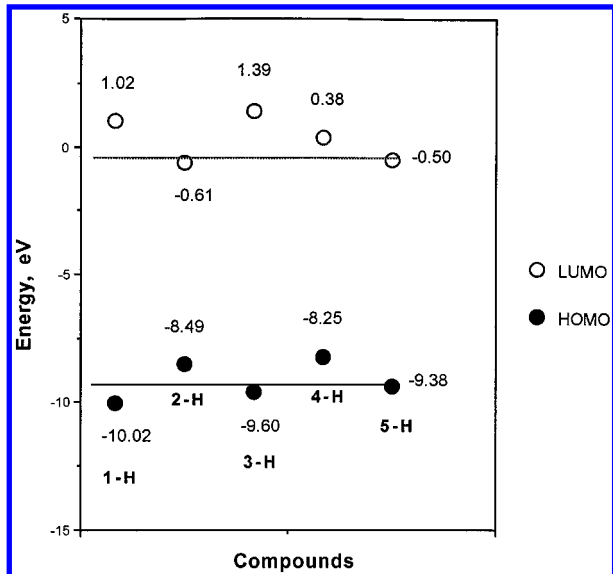
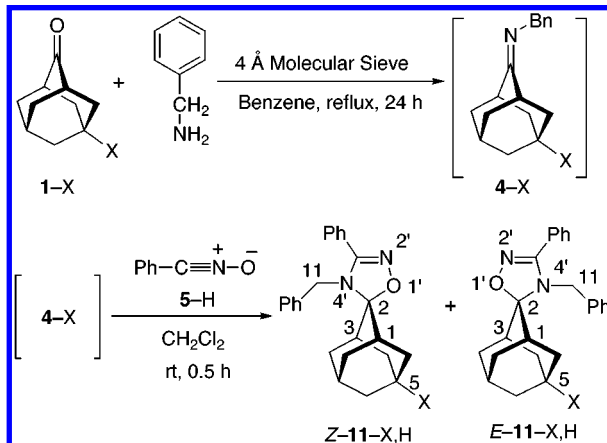


Figure 1. AM1-calculated energies for frontier molecular orbitals of adamantan-2-ones (**1-H**), adamantane-2-thiones (**2-H**), methyleneadamantane (**3-H**), *N*-benzyladamantyl-2-imine (**4-H**), and benzonitrile oxide (**5-H**), where the two lines show the relative energies of dipolarophiles vs those of dipole **5-H**.

Scheme 3



The calculated HOMO and LUMO energies of dipole **5-H** and dipolarophiles **1-H** to **4-H** explain why the reaction of nitrile oxide with adamantanone **1-H** fails even at high temperature and with a long reaction time. On the other hand, one would expect the 1,3-dipolar cycloaddition reaction of **5-H** with *N*-benzyladamantyl-2-imine **4** to proceed very easily, and indeed, the reactions of imines **4-X** with **5-H** in methylene chloride at room temperature proceeded smoothly to completion within 0.5 h (Scheme 3). The imines **4-X** were prepared from corresponding adamantanones (**1-X**) with benzylamine in refluxing benzene. In all cases studied, the yields of *Z*- and *E*-**11-X,H** were 83–92%, but no preference in product configuration was found (Table 3). In a highly exothermic reaction like this, according to the Hammond postulate, the transition state is early, and its structure should resemble that of starting reagents. One would also expect that if the reaction temperature is low enough, the face selectivity should be enhanced; however, the *Z/E*-**11-X,H** product ratio stays constant at ca. 50:50 (\pm 2%) even at -60°C .

The structures of 5-substituted-3'-phenyl-4'-*N*-benzyl-adamantane-2-spiro-5'-(Δ^2 -1',2',4'-oxadiazoline) **11-X,H**

Table 3. 1,3-Dipolar Cycloaddition Reaction of Benzonitrile Oxide (5-H) with 5-Substituted-*N*-benzyladamantane-2-imine (4-X) in Methylene Chloride at Various Temperature for 0.5 h

entry	X	temp, °C	Z:E-11-X,H ^a	yield, %
1	F	rt	51:49	83
2	F	0	51:49	b
3	F	-50	52:48	b
4	F	-60	52:48	b
5	Cl	rt	50:50	87
6	Br	rt	50:50	86
7	Ph	rt	50:50	92

^a The ratios of the *E*- and *Z*-adducts were determined by ¹H NMR. ^b When the ratio was determined, the reaction was not yet complete.

were characterized completely by means of ¹H and ¹³C NMR spectroscopy (Table 4), MS, and HRMS (see Experimental Section). The assignments of configuration were based on the NOE experiments on the **11**-F,H where strong signal enhancements (ca. 6%) were observed between protons on C-11 and C-8, C-10 of the *Z*-**11**-F,H isomer (identified by their small C-F coupling constants) but not between those on C-11 and C-4, C-9. All other adducts were assigned on the basis of the ¹³C NMR additivity scheme, which has been shown to be very successful in the assignment of adamantane structures.⁶⁻⁸ It is interesting to note that *N*-benzyl has a better shielding effect than an oxygen atom directly "above" the flanking methylene carbons in oxadiazolines **11**;¹⁰ thus, C-8 and C-10, which are syn to the *N*-benzyl in the parent **11**-H,H, are shielded by at least 0.67 ppm compared to C-4 and C-9 (Table 4).

Even though the absolute rate equation (eq 1)¹¹ readily permits a systematic study to be made of the temperature dependence of the *Z/E* product,

$$k = RT/Nh \exp(-\Delta G^\ddagger/RT) \quad (1)$$

few such studies have been reported in the adamantane system. For example, although various temperatures were used in the reduction and Grignard reactions of adamantanones **1**-X, no changes in face selectivity were observed.^{1,3} In the course of our study of the 1,3-dipolar cycloaddition reactions, we noticed that temperature variation did cause a substantial face selectivity change in the 1,3-dipolar cycloaddition reactions. Since **2**-Cl and **3**-Cl were available in substantial quantity, their reactions with **6**-H were chosen for a study at various temperatures. The results from temperature effects are summarized in Tables 5 and 6.

Entries 1–4 of both Tables 5 and 6 show the results of generating nitrile oxide (**5**-H) by thermal elimination of HCl from the corresponding hydroximoyl chloride in the absence of triethylamine. At temperatures above 80 °C (but not below), the nitrile oxide can be generated in this way and captured by dipolarophiles **2**-Cl or **3**-Cl. Basically, the product ratio stays constant when nitrile oxide is prepared by this method. At lower temperatures, **5**-H can be generated only in the presence of triethylamine, permitting us to measure the syn/anti product ratios in the wide temperature range of 0–138 °C (entries 5–12 of Tables 5 and 6). The general trend is that as the

(10) For the shielding effect of an oxygen atom on other adamantane-related structures, see ref 6 and references therein.

(11) For a leading reference see Peterson, R. C. *J. Org. Chem.* **1964**, 29, 3133.

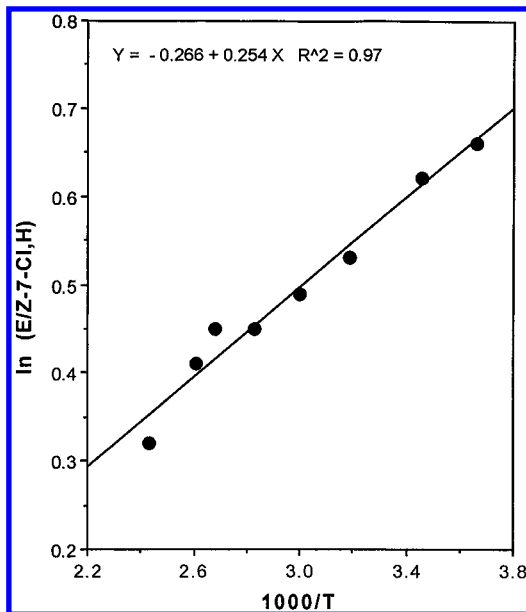


Figure 2. The Arrhenius plot of $\ln(E/Z-7-Cl,H)$ vs $1000/T$ from the 1,3-dipolar cycloaddition reactions of **2**-Cl with benzonitrile oxide **5**-H. The slope is 254 K^{-1} .

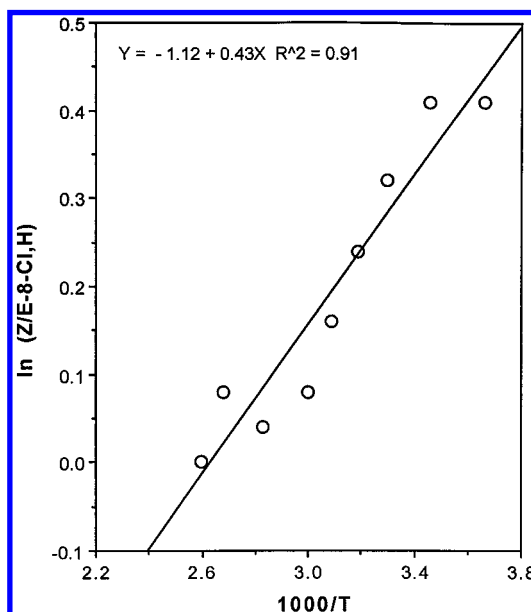


Figure 3. The Arrhenius plot of $\ln(Z/E-8-Cl,H)$ vs $1000/T$ from the 1,3-dipolar cycloaddition reactions of **3**-Cl with benzonitrile oxide **5**-H. The slope is 430 K^{-1} .

temperature increases, the syn/anti face selectivity decreases. Plots of eq 2 (Figure 2 and Figure 3) show that the

$$\ln(k_{\text{syn}}/k_{\text{anti}}) = (\Delta S_{\text{syn}}^\ddagger - \Delta S_{\text{anti}}^\ddagger)/R + (\Delta H_{\text{anti}}^\ddagger - \Delta H_{\text{syn}}^\ddagger)/RT \quad (2)$$

activation enthalpy difference between the two transition states with **2**-Cl is 0.51 kcal/mol and that with **3**-Cl is 0.85 kcal/mol. The syn attack has a lower activation enthalpy than anti attack does, in both cases. The difference in ΔS^\ddagger for **2**-Cl is quite small ($\Delta S_{\text{syn}}^\ddagger - \Delta S_{\text{anti}}^\ddagger \approx -0.53 \text{ eu}$) but larger for **3**-Cl ($\sim -2.23 \text{ eu}$). In that case, the data clearly suggest a reversal of the major and minor isomers at high temperatures. Solutions of pure isoxazo-

Table 4. Calculated^a and Observed^b ¹³C NMR Chemical Shifts of 5-Substituted-3'-phenyl-4'-N-benzyladamantane-2-spiro-5'-(Δ^2 -1'-2'-4'-oxadiazolines)^c

	11-H,H	Z-11-F,H	E-11-F,H	Z-11-Cl,H	E-11-Cl,H	Z-11-Br,H	E-11-Br,H	Z-11-Ph,H	E-11-Ph,H
C ₁ , C ₃	34.43 <i>J</i> = 10.6	36.93 (37.53)	36.94 (37.53) <i>J</i> = 10.2	37.26 (36.53)	36.91 (36.53)	38.10 (38.43)	38.00 (38.43)	34.86 (35.03)	34.57 (35.03)
C ₂	102.42	100.61 (100.62)	100.64 (100.62)	100.40 (100.12)	100.02 (100.12)	100.31 (100.12)	100.11 (100.12)	101.76 (101.52)	101.58 (101.52)
C ₄ , C ₉	34.73 <i>J</i> = 19.5	39.18 (39.73)	38.67 (39.06) <i>J</i> = 19.4	44.14 (44.43)	43.40 (43.76)	45.65 (46.23)	45.11 (45.56)	40.29 (40.13)	39.20 (39.46)
C ₅	26.88 <i>J</i> = 184.3	90.94 (90.68)	91.32 (90.47) <i>J</i> = 184.4	65.95 (66.68)	65.75 (66.47)	62.47 (64.88)	62.69 (64.67)	35.14 (34.58)	35.02 (34.37)
C ₆	37.35 <i>J</i> = 17.6	42.36 (42.35)	42.44 (42.35) <i>J</i> = 16.8	47.29 (47.05)	47.08 (47.05)	48.81 (48.85)	48.70 (48.85)	42.49 (42.75)	42.42 (42.75)
C ₇	26.67 <i>J</i> = 9.9	29.67 (29.77) <i>J</i> = 9.9	29.61 (29.98)	29.89 (28.77)	30.21 (28.98)	30.69 (30.67)	30.61 (30.88)	27.43 (27.27)	26.99 (27.48)
C ₈ , C ₁₀	34.06 <i>J</i> = 2.0	32.39 (32.26)	33.12 (32.94) <i>J</i> = 1.9	32.12 (31.76)	32.49 (32.43)	32.10 (31.76)	32.67 (32.43)	33.16 (33.16)	33.51 (33.83)
C _{3'}	161.28	161.37	161.36	161.39	161.39	161.38	161.30	161.38	161.09
C ₁₁	49.73	49.90	49.79	49.88	49.53	49.83	49.75	49.85	49.37

^a Calculated values are in parentheses. ^b Measured with a Bruker DRX-300 NMR operated at 75.4 MHz and reported in δ units, CDCl₃ (δ 77.00). *J* is in hertz. In the parent compound 11-H,H the oxygen is understood to be syn to C₄ and C₉. ^c The phenyl groups are not shown here but are reported in Experimental Section.

Table 5. Temperature Effects on the Face Selectivity of 1,3-Dipolar Cycloaddition Reaction of Benzonitrile Oxide (5-H) with 5-Chloroadamantane-2-thione (2-Cl) in Toluene or Xylene^a

entry	NEt ₃ (mL)	temp, °C	solvent	time, h	<i>E</i> : <i>Z</i> -7-Cl,H ^b	yield, % ^c
1	—	80	toluene	24	60:40	89
2	—	100	toluene	24	60:40	88
3	—	110	toluene	24	59:41	88
4	—	138	xylene	24	58:42	87
5	0.01	0	toluene	3	65:35	76
6	0.01	0	toluene	24	66:34	78
7	0.01	16	toluene	3	65:35	83
8	0.01	16	toluene	24	65:35	84
9	0.01	40	toluene	3	63:37	70
10	0.01	60	toluene	3	62:38	87
11	0.01	80	toluene	3	61:39	88
12	0.01	100	toluene	3	61:39	87
13	0.01	110	toluene	3	60:40	89
14	0.01	138	xylene	3	58:42	88

^a Fixed concentration of 2-Cl (5 mM) and benzohydroximoyl chloride 6-H (7.5 mM) in toluene or xylene were studied throughout the series. ^b The ratios of the *E*- and *Z*-7-Cl,H were determined by GC. ^c Yields were measured by VPC with an internal standard thioxanthen-9-one (1 mM).

Table 6. Temperature Effects on the Face Selectivity of 1,3-Dipolar Cycloaddition Reaction of Benzonitrile Oxide (5-H) with 5-Chloro-*m*-methyleneadamantane (3-Cl) in Toluene or Xylene for 24 h^a

entry	NEt ₃ (mL)	temp, °C	solvent	<i>Z</i> : <i>E</i> -8-Cl,H ^b	yield, % ^c
1	—	80	toluene	51:49	99 (6)
2	—	100	toluene	51:49	83 (27)
3	—	110	toluene	50:50	93 (99)
4	—	138	xylene	51:49	95 (99)
5	0.01	0	toluene	60:40	89 (88)
6	0.01	16	toluene	60:40	92 (75)
7	0.01	30	toluene	58:42	85 (77)
8	0.01	40	toluene	56:44	87 (82)
9	0.01	50	toluene	54:46	82 (59)
10	0.01	60	toluene	52:48	96 (95)
11	0.01	80	toluene	51:49	83 (82)
12	0.01	100	toluene	52:48	89 (70)
13	0.01	110	toluene	50:50	88 (76)
14	0.01	138	xylene	50:50	91 (89)

^a Fixed concentration of 3-Cl (5.5 mM) and 6-H (8.2 mM) in toluene or xylene were studied throughout the series. ^b The ratios of the *Z*- and *E*-adducts 8-Cl,H were determined by ¹H NMR. ^c Yields were measured by ¹H NMR with 1,4-dioxane as an external standard. Values in parentheses are the percentage conversion.

lines *E*- and *Z*-8-Cl,H in toluene were heated to reflux for 24 h, but no indication of forming the other isomer through cycloreversion was observed; this indicates that

both products are formed in kinetically controlled processes. Although the correlation coefficient of our data in Figure 3 is only 0.91, it is clear that the slopes are positive and the intercepts negative in Figures 2 and 3. The kinetic study shows that the syn-attacks of phenyl nitrile oxides (5-Y) to thione 2-X and methyleneadamantane 3-X (where X is electron withdrawing) have a smaller activation enthalpy (ΔH^\ddagger) and a more negative activation entropy (ΔS^\ddagger) than the anti-attacks. This is consistent with the notion of transition state hyperconjugation model, in which better interactions exist between the more electron-rich anti-periplanar bonds and the σ^* orbital of the incipient bond of dipoles.

Kinetic studies^{5a-c} of 1,3-dipolar additions of nitrones to thiones have revealed that the weakness of the C=S π bond is not responsible for the fast rates; instead, the low HOMO–LUMO energy gap of the C=S π bond was suggested to be the decisive factor. AM1 calculations¹⁵ of the HOMO–LUMO energy of 1–4 (Figure 1) reveal that all the 1,3-dipolar reactions described here are LUMO (dipole)–HOMO (dipolarophile) controlled reactions, i.e. a Sustmann type III reaction,^{4f} and that the rates, which diminish in the order $k(\text{imine}) > k(\text{C=S}) > k(\text{C=CH}_2) \gg k(\text{C=O})$ are consistent with the decreased energy gaps. The energy gaps (ΔE_{II}) between LUMO (dipole)–HOMO (dipolarophile) are as follows: 7.75 eV (4-H), 7.99 eV (2-H), 9.1 eV (3-H) and 9.52 eV (1-H).

The HOMO–LUMO energies of substituted dipolarophiles 2-X to 4-X can also be calculated with the AM1 method (see Supporting Information). All of the 5-substituents except phenyl cause lower HOMO and LUMO energies compared to those of the parent compounds 2-H to 4-H. The calculated LUMO energies of *para*-substituted benzonitrile oxide 5-Y increase with electron-donating substituents (Me and OMe) but decrease with electron-withdrawing groups. The observed small positive values ($\Delta\rho$) in the Hammett plots are consistent with the diminished energy gap for electron-withdrawing *para*-

(12) The author has deposited atomic coordinates for (*Z*)-7-Br (H) with the Cambridge Crystallographic Data Center. The coordinates can be obtained, on request, from the Director, Cambridge Crystallographic Data Centre, 12 Union Road, Cambridge, CB2 1EZ, UK.

(13) (a) Katada, T.; Eguchi, S.; Sasaki, T. *J. Chem. Soc., Perkin Trans. 1* **1984**, 2641. (b) Bonini, B. F.; Maccagnani, G.; Mazzanti, G.; Thijs, L.; Ambrosio, H. P. M. M.; Zwanenburg, B. *J. Chem. Soc., Perkin Trans. 1* **1977**, 1468.

(14) Taguchi, K.; Westheimer, F. H. *J. Org. Chem.* **1971**, 36, 1570.

(15) Dewar, M. J. S.; Zoebisch, E. G.; Healy, E. F.; Stewart, J. J. P. *J. Am. Chem. Soc.* **1985**, 107, 3902.

substituents; e.g., **5**—NO₂ reacts faster and is more selective than **5**—Me when treated with **2**—F (Table 1). The Hammett plot of the reaction of **5**—Y with **3**—F leads to a zero reaction constant ($\Delta\rho = 0$), which indicates that no charge-distribution difference is observed in the two transition states leading to *Z*- and *E*—**8**—F,Y; again, this indicates that electrostatic effects are not important here in these adamantane systems.

Summary

The effects of *para*-substitution of benzonitrile oxides (**5**—Y) on the face selectivity of 1,3-dipolar cycloaddition reactions with **2**—F and **3**—F have been studied. The reaction constant differences $\Delta\rho$ for these reactions are obtained from linear Hammett plots, which give a *small positive* value (+0.12) for thiones (**2**—F) and a *zero* slope for methyleneadamantanes (**3**—F). These small $\Delta\rho$ values imply that the 1,3-dipolar cycloaddition is consistent with a concerted-one-step mechanism with a slightly different charge imbalance in the transition states.

Effects of temperature variation on the *Z/E* product ratios of the 1,3-dipolar cycloaddition reactions of **2**—Cl and **3**—Cl with parent nitrile oxide **5**—H provide us, for the first time, with the activation enthalpy and entropy differences between the two transition states of the syn- and anti-face attacks. The syn-attacks of the dipoles (**5**—X) on thiones **2**—X and methyleneadamantane **3**—X have a smaller activation enthalpy (ΔH^\ddagger) and a more negative activation entropy (ΔS^\ddagger) than the anti-attacks.

AM1 calculations of the HOMO–LUMO energies of **1**–**5** reveal that all the 1,3-dipolar reactions described here are LUMO (dipole)–HOMO (dipolarophile) controlled reactions; the rates decrease in the order $k(\text{imine}) > k(\text{C=S}) > k(\text{C=CH}_2) \gg k(\text{C=O})$, consistent with decreased energy gaps.

Experimental Section

¹H NMR spectra were measured on 300 and 400 MHz spectrometers. The data reported were recorded at 300 MHz. Natural abundance ¹³C NMR spectra were measured using pulsed Fourier transform, on either a Varian Unity-300 or Bruker DRX-300 high-resolution NMR spectrometer operating at 75.4 MHz. Broad-band decoupling, DEPT and 2D H,C-COSY experiments were carried to simplify spectra and aid peak identification. Chemical shifts are given in ppm and J in hertz for both nuclei, with the solvent (usually CDCl₃) peak as an internal standard. The reference peak for ¹³C is δ 77.00, which is set at the center peak of CDCl₃, and for ¹H it is δ 7.25 of CHCl₃. Gas chromatographic analyses were carried out on an instrument equipped with a flame ionization detector and a reporting integrator. The capillary column employed included HP-1 cross-linked methylsilicone (SE-30, 25 m) and carbowax column (25 m). GC/MS spectral analyses were carried out with EI (at 70 eV).

General Procedure for the Synthesis of 5-Fluoro-3'-*para*-substituted-phenyladamantane-2-spiro-5'-(Δ^2 -1',4',2'-oxathiazolines) (*E*- and *Z*—7**—F,Y).** To a well-stirred solution of **2**—F (100 mg, 0.5 mmol) and **6**—Y (0.75 mmol) in anhydrous methylene chloride (10 mL) was added an excess of triethylamine (0.75 mol equiv). After being stirred for 3 h at room temperature, the mixture was washed with water and dried (MgSO₄); after filtration and solvent evaporation, the solid residue was purified on a silica gel column by elution with *n*-hexane/methylene chloride to give *E*- and *Z*—**7**—F,Y. The isolated yields based on converted **2**—F are as follows: **7**—F, 85%; **7**—F,Cl 94%; **7**—F,Br 78%; **7**—F,CN 89%; **7**—F,NO₂ 88%; **7**—F,Me 80%; **7**—F,OMe 86%.

***E*—**7**—F,F:** colorless solid; mp 90–91.5 °C; δ _H 1.70–2.00 (m, 8 H), 2.20–2.30 (m, 1 H), 2.40–2.60 (m, 2 H), 2.70 (bs, 2 H), 7.00–7.15 (m, 2 H), 7.60–7.75 (m, 2 H); δ _C 29.79 (C₇, J = 9.8 Hz), 35.68 (C_{8,10}, J = 1.8 Hz), 38.31 (C_{4,9}, J = 19.8 Hz), 42.02 (C_{1,3}, J = 10.2 Hz), 42.19 (C₆, J = 16.1 Hz), 90.10 (C₅, J = 185.2 Hz), 109.89 (C₂, J = 1.5 Hz), 115.92 (C_m, J = 22.1 Hz), 124.70 (C_i, J = 3.5 Hz), 129.69 (C_o, J = 8.6 Hz), 155.22 (C₃), 164.17 (C_p, J = 252.1 Hz); MS (EI, *m/z* 321 (M⁺, 42), 184 (43), 168 (6), 153 (100), 97 (14); HRMS calcd for C₁₇H₁₇OSF₂N: C, 63.53; H, 5.33; N, 4.36, found C, 63.66; H, 5.40; N, 4.26.

***Z*—**7**—F,F:** colorless solid; mp 129.5–131.5 °C; δ _H 1.50–1.70 (m, 2 H), 1.85–2.18 (m, 6 H), 2.20–2.35 (m, 3 H), 2.66 (bs, 2 H), 7.00–7.15 (m, 2 H), 7.60–7.75 (m, 2 H); δ _C 29.09 (C₇, J = 9.9 Hz), 32.11 (C_{8,10}, J = 1.8 Hz), 41.47 (C_{4,9}, J = 19.7 Hz), 41.72 (C_{1,3}, J = 10.5 Hz), 42.20 (C₆, J = 17.1 Hz), 90.52 (C₅, J = 185.5 Hz), 110.40 (C₂, J = 1.3 Hz), 115.92 (C_m, J = 22.1 Hz), 124.68 (C_i, J = 3.5 Hz), 129.70 (C_o, J = 8.6 Hz), 155.48 (C₃), 164.18 (C_p, J = 252.2 Hz); MS (EI, *m/z* 321 (M⁺, 36), 258 (25), 214 (32), 184 (29), 153 (100), 137 (37), 109 (18); HRMS calcd for C₁₇H₁₇OSF₂N 321.1000, found 321.0995.

***E*—**7**—F,Cl:** colorless solid; mp 157–158.5 °C; δ _H 1.60–2.00 (m, 8 H), 2.20–2.30 (m, 1 H), 2.40–2.60 (m, 2 H), 2.70 (bs, 2 H), 7.30–7.40 (m, 2 H), 7.55–7.65 (m, 2 H); δ _C 29.77 (C₇, J = 9.9 Hz), 35.67 (C_{8,10}, J = 1.7 Hz), 38.30 (C_{4,9}, J = 19.8 Hz), 42.06 (C_{1,3}, J = 10.2 Hz), 42.18 (C₆, J = 17.9 Hz), 90.06 (C₅, J = 185.0 Hz), 111.08 (C₂), 126.97 (C_i), 128.85 (C_m), 129.00 (C_o), 136.94 (C_p), 155.22 (C₃); MS (EI, *m/z* 339 (M⁺ + 2, 18), 337 (M⁺, 46), 184 (50), 171 (37), 169 (100), 97 (15); HRMS calcd for C₁₇H₁₇OSFN³⁵Cl 337.0705, found 337.0705.

***Z*—**7**—F,Cl:** colorless solid; mp 154–156 °C; δ _H 1.50–1.60 (m, 2 H), 1.85–2.15 (m, 6 H), 2.15–2.30 (m, 3 H), 2.66 (bs, 2 H), 7.30–7.40 (m, 2 H), 7.50–7.65 (m, 2 H); δ _C 29.10 (C₇, J = 9.7 Hz), 32.12 (C_{8,10}, J = 2.0 Hz), 41.47 (C_{4,9}, J = 19.7 Hz), 41.78 (C_{1,3}, J = 10.5 Hz), 42.20 (C₆, J = 17.2 Hz), 90.47 (C₅, J = 185.6 Hz), 110.58 (C₂), 126.97 (C_i), 128.87 (C_m), 129.01 (C_o), 136.97 (C_p), 155.47 (C₃); MS (EI, *m/z* 339 (M⁺ + 2, 17), 337 (M⁺, 44), 184 (74), 171 (38), 169 (100), 97 (15); HRMS calcd for C₁₇H₁₇OSFN³⁵Cl 337.0705, found 337.0703.

***E*—**7**—F,Br:** colorless solid; mp 176–176.5 °C; δ _H 1.70–2.05 (m, 8 H), 2.20–2.35 (m, 1 H), 2.40–2.60 (m, 2 H), 2.70 (bs, 2 H), 7.54 (s, 4 H); δ _C 29.78 (C₇, J = 9.9 Hz), 35.68 (C_{8,10}, J = 1.9 Hz), 38.31 (C_{4,9}, J = 19.8 Hz), 42.08 (C_{1,3}, J = 10.2 Hz), 42.18 (C₆, J = 18.1 Hz), 90.03 (C₅, J = 185.5 Hz), 110.13 (C₂), 125.28 (C_p), 127.44 (C_i), 129.03 (C_m), 131.96 (C_o), 155.29 (C₃); MS (EI) *m/z* 383 (M⁺ + 2, 46), 381 (M⁺, 44), 215 (100), 213 (98), 184 (67), 97 (22); HRMS calcd for C₁₇H₁₇OSFN⁷⁹Br 381.0154, found 381.0200.

***Z*—**7**—F,Br:** colorless solid; mp 181–181.5 °C; δ _H 1.55–1.65 (m, 2 H), 1.90–2.20 (m, 6 H), 2.27 (bs, 3 H), 2.66 (bs, 2 H), 7.54 (s, 4 H); δ _C 29.12 (C₇, J = 9.9 Hz), 32.14 (C_{8,10}, J = 1.6 Hz), 41.50 (C_{4,9}, J = 19.9 Hz), 41.82 (C_{1,3}, J = 10.4 Hz), 42.23 (C₆, J = 17.0 Hz), 90.46 (C₅, J = 186.0 Hz), 110.66 (C₂), 125.32 (C_p), 127.46 (C_i), 129.07 (C_m), 131.99 (C_o), 155.57 (C₃); MS (EI, *m/z* 383 (M⁺ + 2, 55), 381 (M⁺, 52), 215 (100), 213 (96), 184 (54), 97 (29); HRMS calcd for C₁₇H₁₇OSFN⁷⁹Br 381.0154, found 381.0194.

***E*—**7**—F,CN:** colorless solid; mp 186–187.5 °C; δ _H 1.70–1.92 (m, 6 H), 1.96 (bs, 1 H), 2.40–2.60 (m, 2 H), 2.70 (bs, 2 H), 7.60–7.80 (m, 4 H); δ _C 29.67 (C₇, J = 10.0 Hz), 35.61 (C_{8,10}, J = 1.9 Hz), 38.24 (C_{4,9}, J = 19.9 Hz), 42.10 (C₆, J = 19.4 Hz), 42.17 (C_{1,3}, J = 10.1 Hz), 89.89 (C₅, J = 185.3 Hz), 111.10 (C₂), 114.22 (C_p), 118.03 (C_{CN}), 128.06 (C_o), 132.44 (C_m), 132.71 (C_i), 155.29 (C₃); MS (EI, *m/z* 328 (M⁺, 100), 184 (88), 168 (65), 160 (71), 128 (16), 97 (38); HRMS calcd for C₁₈H₁₇OSFN₂ 328.1047, found 328.1051. Anal. Calcd for C₁₈H₁₇OSFN₂: C, 65.83; H, 5.22; N, 8.53, found C, 65.43; H, 5.20; N, 8.42.

***Z*—**7**—F,CN:** colorless solid; mp 198–198.5 °C; δ _H 1.55–1.65 (m, 2 H), 1.90–2.15 (m, 6 H), 2.20–2.30 (m, 3 H), 2.55–2.70 (m, 2 H), 7.60–7.80 (m, 4 H); δ _C 29.02 (C₇, J = 9.7 Hz), 32.09 (C_{8,10}, J = 1.9 Hz), 41.40 (C_{4,9}, J = 19.9 Hz), 41.90 (C_{1,3}, J = 10.5 Hz), 42.13 (C₆, J = 17.1 Hz), 90.31 (C₅, J = 185.7 Hz), 110.62 (C₂), 114.27 (C_p), 118.04 (C_{CN}), 128.09 (C_o), 132.46 (C_m), 132.72 (C_i), 154.82 (C₃); MS (EI, *m/z* 328 (M⁺, 43), 184 (51), 168 (70), 128 (100), 97 (41); HRMS calcd for C₁₈H₁₇OSFN₂

328.1047, found 328.1043. Anal. Calcd for $C_{18}H_{17}OSFN_2$: C, 65.83; H, 5.22; N, 8.53, found C, 65.40; H, 5.21; N, 8.49.

E-7-F,NO₂: colorless solid; mp 243–243.5 °C; δ_H 1.70–1.95 (m, 6 H), 1.98 (bs, 2 H), 2.25–2.35 (m, 1 H), 2.53 (bs, 2 H), 2.73 (bs, 2 H), 7.80–7.90 (m, 2 H), 8.20–8.30 (m, 2 H); δ_C 29.67 (C_7 , J = 10.0 Hz), 35.63 ($C_{8,10}$, J = 1.5 Hz), 38.25 ($C_{4,9}$, J = 19.9 Hz), 42.10 (C_6 , J = 18.0 Hz), 42.22 ($C_{1,3}$, J = 10.2 Hz), 89.90 (C_5 , J = 185.3 Hz), 111.40 (C_2), 123.96 (C_6), 128.41 (C_m), 134.43 (C_4), 148.90 (C_p), 155.29 (C_3); MS (EI, m/z) 348 (M^+ , 77), 184 (100), 168 (63), 150 (30), 97 (59), 79 (30); HRMS calcd for $C_{17}H_{17}O_3SFN_2$ 348.0945, found 348.0952. Anal. Calcd for $C_{17}H_{17}O_3SFN_2$: C, 58.61; H, 4.92; N, 8.04, found C, 58.60; H, 5.03; N, 7.96.

Z-7-F,NO₂: colorless solid; mp 242–243.5 °C; δ_H 1.61 (bs, 1 H), 1.65 (bs, 1 H), 1.90–2.15 (m, 6 H), 2.20–2.35 (m, 3 H), 2.69 (bs, 2 H), 7.80–7.90 (m, 2 H), 8.20–8.30 (m, 2 H); δ_C 29.03 (C_7 , J = 9.9 Hz), 32.10 ($C_{8,10}$, J = 1.7 Hz), 41.41 ($C_{4,9}$, J = 19.9 Hz), 41.95 ($C_{1,3}$, J = 10.6 Hz), 42.14 (C_6 , J = 17.4 Hz), 90.31 (C_5 , J = 185.7 Hz), 111.92 (C_2), 123.97 (C_6), 128.44 (C_m), 134.44 (C_4), 148.93 (C_p), 154.48 (C_3); MS (EI, m/z) 348 (M^+ , 88), 184 (100), 168 (79), 150 (35), 97 (63), 79 (31); HRMS calcd for $C_{17}H_{17}O_3SFN_2$ 348.0945, found 348.0943.

E-7-F,OMe: colorless solid; mp 147–148.5 °C; δ_H 1.75–1.90 (m, 6 H), 1.90–2.00 (m, 2 H), 2.20–2.35 (m, 1 H), 2.50–2.60 (m, 2 H), 2.69 (bs, 2 H), 3.84 (s, 3 H), 6.85–7.00 (m, 2 H), 7.55–7.65 (m, 2 H); δ_C 29.85 (C_7 , J = 9.8 Hz), 35.71 ($C_{8,10}$, J = 1.7 Hz), 38.35 ($C_{4,9}$, J = 19.6 Hz), 41.94 ($C_{1,3}$, J = 10.2 Hz), 42.23 (C_6 , J = 17.9 Hz), 55.40 (C_{MeO}), 90.21 (C_5 , J = 185.0 Hz), 109.03 (C_2), 114.09 (C_m), 120.93 (C_4), 129.26 (C_6), 155.98 (C_3), 161.68 (C_p); MS (EI, m/z) 333 (M^+ , 52), 317 (6), 165 (100), 149 (55), 133 (29), 97 (16); HRMS calcd for $C_{18}H_{20}O_2SFN$ 333.1200, found 333.1195. Anal. Calcd for $C_{18}H_{20}O_2SFN$: C, 64.84; H, 6.05; N, 4.20, found C, 64.99; H, 6.08; N, 4.17.

Z-7-F,OMe: colorless solid; mp 109–111 °C; δ_H 1.57 (bs, 1 H), 1.61 (bs, 1 H), 1.90–2.20 (m, 6 H), 2.20–2.35 (m, 3 H), 2.67 (bs, 2 H), 3.84 (s, 3 H), 6.85–6.95 (m, 2 H), 7.55–7.70 (m, 2 H); δ_C 29.12 (C_7 , J = 9.9 Hz), 32.11 ($C_{8,10}$, J = 1.9 Hz), 41.49 ($C_{4,9}$, J = 19.7 Hz), 41.58 ($C_{1,3}$, J = 10.4 Hz), 42.21 (C_6 , J = 17.0 Hz), 55.39 (C_{MeO}), 90.68 (C_5 , J = 185.1 Hz), 109.50 (C_2), 114.06 (C_m), 120.85 (C_4), 129.27 (C_6), 155.28 (C_3), 161.65 (C_p); MS (EI, m/z) 333 (M^+ , 53), 298 (6), 238 (23), 165 (100), 150 (51), 97 (9); HRMS calcd for $C_{18}H_{20}O_2SFN$ 333.1200, found 333.1202. Anal. Calcd for $C_{18}H_{20}O_2SFN$: C, 64.84; H, 6.05; N, 4.20, found C, 64.76; H, 6.05; N, 4.62.

E-7-F,Me: colorless solid; mp 104–106 °C; δ_H 1.70–1.90 (m, 6 H), 1.90–2.00 (m, 2 H), 2.20–2.30 (m, 1 H), 2.38 (s, 3 H), 2.45–2.60 (m, 2 H), 2.70 (bs, 2 H), 7.15–7.25 (m, 2 H), 7.50–7.60 (m, 2 H); δ_C 21.46 (C_{CH_3}), 29.84 (C_7 , J = 9.9 Hz), 35.69 ($C_{8,10}$, J = 1.8 Hz), 38.34 ($C_{4,9}$, J = 19.6 Hz), 42.01 ($C_{1,3}$, J = 10.2 Hz), 42.23 (C_6 , J = 18.0 Hz), 90.16 (C_5 , J = 185.1 Hz), 109.11 (C_2), 125.66 (C_4), 127.60 (C_6), 129.39 (C_m), 141.35 (C_p), 156.28 (C_3); MS (EI, m/z) 317 (M^+ , 56), 206 (11), 184 (34), 149 (100), 91 (54), 79 (13); HRMS calcd for $C_{18}H_{20}OSFN$ 317.1251, found 317.1243. Anal. Calcd for $C_{18}H_{20}OSFN$: C, 68.11; H, 6.35; N, 4.41, found C, 68.01; H, 6.33; N, 4.66.

Z-7-F,Me: colorless solid; mp 115–117 °C; δ_H 1.50–1.68 (m, 2 H), 1.90–2.18 (m, 6 H), 2.20–2.35 (m, 3 H), 2.38 (s, 3 H), 2.66 (bs, 2 H), 7.15–7.25 (m, 2 H), 7.50–7.60 (m, 2 H); δ_C 21.49 (C_{CH_3}), 29.16 (C_7 , J = 9.7 Hz), 32.14 ($C_{8,10}$, J = 2.0 Hz), 41.52 ($C_{4,9}$, J = 19.7 Hz), 41.72 ($C_{1,3}$, J = 10.6 Hz), 42.26 (C_6 , J = 17.0 Hz), 90.63 (C_5 , J = 185.5 Hz), 109.63 (C_2), 125.64 (C_4), 127.63 (C_6), 129.41 (C_m), 141.40 (C_p), 156.59 (C_3); MS (EI, m/z) 317 (M^+ , 31), 266 (17), 206 (100), 184 (16), 149 (55), 91 (28), 79 (6); HRMS calcd for $C_{18}H_{20}OSFN$ 317.1251, found 317.1248.

X-ray Structure Analysis of Z-7-Br,H. A colorless prism crystal of $C_{17}H_{18}ONBrS$ was crystallized from 30% methylene chloride in hexanes. Its structure was determined by means of single-crystal X-ray analysis on a Rigaku AFC6S diffractometer with a graphite monochromated Mo-K α (λ = 0.71069 Å) radiation at 296 ± 1 K, with an ω –2 θ type scan at $16^\circ/\text{min}$ (in ω). The crystals are monoclinic, with space group $P2_1/c$ (14) and unit cell dimensions a = 16.844(5) Å, b = 24.537(4) Å, c = 10.048(4) Å, β = 108.48(3)°, V = 1600(1) Å³, Z = 4, $\rho_{\text{calcd}} = 1.512$ g cm⁻³, crystal size (mm) 0.33 × 0.41 × 0.48, $\mu(\text{Mo K}\alpha)$ = 27.05 cm⁻¹, $F(000)$ = 744.00, 2688 reflections, 2466 unique

reflections, 772 with $I > 3.00\sigma(I)$ and with 190 variable parameters. The non-hydrogen atoms were refined anisotropically. Hydrogen atoms were included but not refined. The model was finally refined by the full-matrix least-squares methods with weight $\omega = 1/[o^2(F_0)]$ to final R values of 0.075 and $R_w = 0.0351$ (for details, see Supporting Information).¹²

General Procedure for the Synthesis of 5-Fluoro-3'-para-substituted-4'-hydrospiro[adamantane-2:5'-Δ²-isoxazolines] (E- and Z-8-F,Y). **E**- and **Z-8-F,Y** were synthesized by the use of a procedure similar to that of Zwanenburg et al.¹³ An excess of triethylamine (1.5 mol equiv) was added to a well-stirred solution of the **3-F**^{1c} (50 mg, 0.3 mmol) and **6-Y** (1.5 mol equiv) in anhydrous THF (10 mL). The mixture was stirred at reflux for 24 h, diluted with methylene chloride, washed with water, and dried with MgSO₄. After filtration and solvent evaporation, the residue was purified on a silica gel column by elution with *n*-hexane/methylene chloride to give two isomeric adducts **E**- and **Z-8-F,Y**. The isolated yields based on converted starting materials **3-F** are as follows: **8-F,F** 85%, **8-F,Cl** 79%, **8-F,Br** 82%, **8-F,CN** 83%, **8-F,NO₂** 88%, **8-F,Me** 77%, **8-F,OMe** 81%.

Z-8-F,F: colorless solid; mp 160.5–161.5 °C; δ_H 1.65–1.85 (m, 6 H), 1.90–2.00 (m, 2 H), 2.20–2.30 (m, 3 H), 2.40–2.60 (m, 2 H), 3.14 (s, 2 H), 7.00–7.15 (m, 2 H), 7.60–7.70 (m, 2 H); δ_C 29.76 (C_7 , J = 9.9 Hz), 33.93 ($C_{8,10}$, J = 1.6 Hz), 38.23 ($C_{4,9}$, J = 19.2 Hz), 39.86 ($C_{1,3}$, J = 10.4 Hz), 42.33 (C_6 , J = 17.8 Hz), 43.11 (C_4), 89.39 (C_2), 90.88 (C_5 , J = 184.5 Hz), 115.82 (C_m , J = 21.9 Hz), 126.22 (C_i , J = 2.9 Hz), 128.27 (C_o , J = 8.5 Hz), 155.05 (C_3), 163.64 (C_p , J = 250.6 Hz); MS (EI, m/z) 303 (M^+ , 100), 286 (35), 135 (24), 79 (9); HRMS calcd for $C_{18}H_{19}NOF_2$ 303.1438, found 303.1441. Anal. Calcd for $C_{18}H_{19}NOF_2$: C, 71.27; H, 6.31; N, 4.59.

E-8-F,F: colorless solid; mp 157–158 °C; δ_H 1.52 (bs, 1 H), 1.56 (bs, 1 H), 1.95 (bs, 6 H), 2.15–2.30 (m, 5 H), 3.19 (s, 2 H), 7.00–7.15 (m, 2 H), 7.60–7.70 (m, 2 H); δ_C 29.37 (C_7 , J = 9.8 Hz), 31.69 ($C_{8,10}$, J = 1.9 Hz), 39.31 ($C_{1,3}$, J = 10.1 Hz), 40.05 ($C_{4,9}$, J = 18.9 Hz), 42.40 (C_6 , J = 16.9 Hz), 44.18 (C_4), 89.72 (C_2), 90.98 (C_5 , J = 185.0 Hz), 115.83 (C_m , J = 21.9 Hz), 126.20 (C_i , J = 3.3 Hz), 128.28 (C_o , J = 8.4 Hz), 155.20 (C_3), 163.66 (C_p , J = 250.6 Hz); MS (EI, m/z) 303 (M^+ , 100), 286 (33), 135 (26), 79 (9); HRMS calcd for $C_{18}H_{19}NOF_2$ 303.1438, found 303.1442. Anal. Calcd for $C_{18}H_{19}NOF_2$: C, 71.27; H, 6.31; N, 4.62, found C, 71.11; H, 6.36; N, 4.62.

Z-8-F,Cl: colorless solid; mp 202.5–203 °C; δ_H 1.65–1.85 (m, 6 H), 1.90–2.00 (m, 2 H), 2.20–2.30 (m, 3 H), 2.40–2.55 (m, 2 H), 3.13 (s, 2 H), 7.30–7.40 (m, 2 H), 7.55–7.65 (m, 2 H); δ_C 29.76 (C_7 , J = 9.8 Hz), 33.93 ($C_{8,10}$, J = 1.7 Hz), 38.22 ($C_{4,9}$, J = 19.3 Hz), 39.88 ($C_{1,3}$, J = 10.3 Hz), 42.33 (C_6 , J = 17.9 Hz), 42.89 (C_4 , J = 2.0 Hz), 89.61 (C_2), 90.86 (C_5 , J = 184.3 Hz), 127.58 (C_0), 128.48 (C_i), 128.96 (C_m), 135.86 (C_p), 155.08 (C_3); MS (EI, m/z) 321 ($M^+ + 2$, 38), 319 (M^+ , 100), 302 (38), 151 (25), 79 (12); HRMS calcd for $C_{18}H_{19}NOF^{35}Cl$ 319.1141, found 319.1138.

E-8-F,Cl: colorless solid; mp 191.5–192 °C; δ_H 1.52 (bs, 1 H), 1.56 (bs, 1 H), 1.85–2.00 (m, 6 H), 2.10–2.35 (m, 5 H), 3.18 (s, 2 H), 7.30–7.40 (m, 2 H), 7.55–7.65 (m, 2 H); δ_C 29.33 (C_7 , J = 9.9 Hz), 31.65 ($C_{8,10}$, J = 2.0 Hz), 39.29 ($C_{1,3}$, J = 10.0 Hz), 40.00 ($C_{4,9}$, J = 19.0 Hz), 42.36 (C_6 , J = 16.8 Hz), 43.93 (C_4), 89.94 (C_2), 90.96 (C_5 , J = 184.8 Hz), 127.57 (C_0), 128.40 (C_i), 128.94 (C_m), 135.85 (C_p), 155.24 (C_3); MS (EI, m/z) 321 ($M^+ + 2$, 35), 319 (M^+ , 100), 302 (39), 151 (22), 79 (11); HRMS calcd for $C_{18}H_{19}NOFCl$: C, 67.60; H, 5.99; N, 4.38, found C, 67.25; H, 6.05; N, 4.34.

Z-8-F,Br: colorless solid; mp 206–207 °C; δ_H 1.60–1.85 (m, 6 H), 1.90–2.00 (m, 2 H), 2.23 (bs, 3 H), 2.40–2.55 (m, 2 H), 3.13 (s, 2 H), 7.45–7.60 (m, 4 H); δ_C 29.76 (C_7 , J = 9.9 Hz), 33.92 ($C_{8,10}$, J = 2.1 Hz), 38.22 ($C_{4,9}$, J = 19.0 Hz), 39.87 ($C_{1,3}$, J = 10.4 Hz), 42.33 (C_6 , J = 17.6 Hz), 42.84 (C_4), 87.82 (C_2), 90.87 (C_5 , J = 183.4 Hz), 124.16 (C_p), 127.80 (C_0), 128.91 (C_i), 131.91 (C_m), 155.18 (C_3); MS (EI, m/z) 365 ($M^+ + 2$, 100), 363 (M^+ , 100), 348 (27), 346 (27), 197 (18), 79 (10); HRMS calcd for $C_{18}H_{19}NOF^7Br$ 363.0635, found 363.0635. Anal. Calcd for

C₁₈H₁₉NOFBr: C, 59.35; H, 5.26; N, 3.84, found C, 59.61; H, 5.28; N, 3.71.

E-8-F,Br: colorless solid; mp 177–178.5 °C; δ_H 1.52 (bs, 1 H), 1.56 (bs, 1 H), 1.90–2.00 (m, 6 H), 2.15–2.30 (m, 5 H), 3.18 (s, 2 H), 7.50–7.55 (m, 4 H); δ_C 29.35 (C₇, J = 9.7 Hz), 31.67 (C_{8,10}, J = 1.9 Hz), 39.31 (C_{1,3}, J = 10.1 Hz), 40.02 (C_{4,9}, J = 18.9 Hz), 42.38 (C₆, J = 16.7 Hz), 43.89 (C_{4'}), 89.72 (C₂), 90.95 (C₅, J = 184.8 Hz), 124.18 (C_p), 127.81 (C₀), 128.88 (C_i), 131.92 (C_m), 155.33 (C₃); MS (EI, m/z) 365 (M⁺ + 2, 100), 363 (M⁺, 100), 348 (25), 346 (26), 197 (19), 79 (11); HRMS calcd for C₁₈H₁₉NOF⁷⁹Br 363.0635, found 363.0640. Anal. Calcd for C₁₈H₁₉NOFBr: C, 59.35; H, 5.26; N, 3.84, found C, 59.65; H, 5.27; N, 3.72.

Z-8-F,CN: could not obtained in pure form. δ_H 1.65–1.90 (m, 6 H), 1.96 (bs, 2 H), 2.27 (bs, 3 H), 2.45–2.60 (m, 2 H), 3.21 (s, 2 H), the aromatic region overlapped with impurities; δ_C 29.72 (C₇, J = 10.2 Hz), 33.90 (C_{8,10}), 38.19 (C_{4,9}, J = 19.2 Hz), 39.90 (C_{1,3}, J = 10.2 Hz), 42.28 (C₆, J = 17.8 Hz), 42.58 (C_{4'}), 90.38 (C₂), 90.75 (C₅, J = 184.7 Hz), the aromatic region overlapped with impurities.

E-8-F,CN: colorless solid; mp 242–243 °C; δ_H 1.50–165 (m, 2 H), 1.90–2.00 (m, 6 H), 2.15–2.35 (m, 5 H), 3.19 (s, 2 H), 7.60–7.70 (m, 2 H), 7.70–7.80 (m, 2 H); δ_C 29.29 (C₇, J = 9.8 Hz), 31.63 (C_{8,10}, J = 1.7 Hz), 39.34 (C_{1,3}, J = 10.1 Hz), 39.96 (C_{4,9}, J = 19.0 Hz), 42.32 (C₆, J = 16.7 Hz), 43.47 (C_{4'}), 90.82 (C₅, J = 185.2 Hz), 90.93 (C₂), 113.23 (C_p), 118.36 (CN), 126.79 (C₀), 132.48 (C_m), 134.22 (C_i), 154.87 (C₃); MS (FAB⁺, m/z) 311 (M⁺ + 1, 12), 307 (12), 154 (100), 136 (83), 77 (35); HRMS (FAB⁺) calcd for C₁₉H₁₉N₂OF 311.1569, found 311.1557.

Z-8-F,NO₂: mp 298–299 °C but color turned from none to brown at 253 °C; δ_H 1.65–1.85 (m, 6 H), 1.96 (bs, 2 H), 2.26 (bs, 3 H), 2.50 (bs, 2 H), 3.18 (s, 2 H), 7.78–7.88 (m, 2 H), 8.20–8.30 (m, 2 H); δ_C 29.69 (C₇, J = 9.7 Hz), 33.89 (C_{8,10}, J = 2.0 Hz), 38.16 (C_{4,9}, J = 19.4 Hz), 39.00 (C_{1,3}, J = 10.4 Hz), 42.27 (C₆, J = 18.0 Hz), 42.48 (C_{4'}, J = 1.9 Hz), 90.66 (C₅, J = 184.9 Hz), 90.88 (C₂), 124.00 (C_m), 127.03 (C₀), 136.06 (C_i), 148.35 (C_p), 154.45 (C₃); MS (EI, m/z) 330 (M⁺, 100), 313 (37), 300 (18), 162 (18), 97 (22), 79 (25); HRMS calcd for C₁₈H₁₉N₂O₃F 330.1381, found 330.1378.

E-8-F,NO₂: colorless solid; mp 290.291 °C; δ_H 1.50–1.65 (m, 2 H), 1.97 (bs, 6 H), 2.15–2.35 (m, 5 H), 3.23 (s, 2 H), 7.75–7.88 (m, 2 H), 8.20–8.30 (m, 2 H); δ_C 29.29 (C₇, J = 9.9 Hz), 31.63 (C_{8,10}, J = 2.0 Hz), 39.36 (C_{1,3}, J = 10.0 Hz), 39.96 (C_{4,9}, J = 19.2 Hz), 42.32 (C₆, J = 16.6 Hz), 43.53 (C_{4'}), 90.77 (C₅, J = 185.0 Hz), 91.19 (C₂), 124.00 (C_m), 127.04 (C₀), 136.02 (C_i), 148.35 (C_p), 154.63 (C₃); MS (EI, m/z) 330 (M⁺, 100), 313 (19), 300 (13), 162 (25), 97 (16), 79 (16); HRMS calcd for C₁₈H₁₉N₂O₃F 330.1381, found 330.1372.

Z-8-F,OMe: colorless solid; mp 161.5–163 °C; δ_H 1.65–1.85 (m, 6 H), 1.94 (bs, 2 H), 2.22 (bs, 3 H), 2.50 (bs, 2 H), 3.14 (s, 2 H), 3.83 (s, 3 H), 6.85–6.95 (m, 2 H), 7.55–7.65 (m, 2 H); δ_C 29.77 (C₇, J = 10.0 Hz), 33.92 (C_{8,10}, J = 1.6 Hz), 38.24 (C_{4,9}, J = 19.0 Hz), 39.82 (C_{1,3}, J = 10.4 Hz), 42.33 (C₆, J = 17.8 Hz), 43.22 (C_{4'}), 55.32 (C_{OMe}), 88.73 (C₂), 91.01 (C₅, J = 184.5 Hz), 114.04 (C_m), 122.48 (C_i), 127.84 (C₀), 155.60 (C₃), 160.87 (C_p); MS (EI, m/z) 315 (M⁺, 100), 298 (25), 285 (5), 174 (10), 147 (15), 97 (8), 77 (11); HRMS calcd for C₁₉H₂₂NO₂F 315.1636, found 315.1625.

E-8-F,OMe: colorless solid; mp 170–172 °C; δ_H 1.50 (bs, 1 H), 1.55 (bs, 1 H), 1.96 (bs, 6 H), 2.10–2.30 (m, 5 H), 3.18 (s, 2 H), 3.84 (s, 3 H), 6.90–6.95 (m, 2 H), 7.55–7.65 (m, 2 H); δ_C 29.41 (C₇, J = 9.9 Hz), 31.72 (C_{8,10}, J = 1.8 Hz), 39.29 (C_{1,3}, J = 10.1 Hz), 40.08 (C_{4,9}, J = 18.9 Hz), 42.43 (C₆, J = 16.7 Hz), 44.35 (C_{4'}), 55.35 (C_{OMe}), 89.11 (C₂), 91.16 (C₅, J = 184.6 Hz), 114.08 (C_m), 122.49 (C_i), 127.88 (C₀), 155.78 (C₃), 160.92 (C_p); MS (EI, m/z) 315 (M⁺, 100), 298 (6), 285 (4), 174 (12), 147 (18), 97 (10), 77 (11); HRMS calcd for C₁₉H₂₂NO₂F 315.1636, found 315.1628.

Z-8-F,Me: colorless solid; mp 127–128 °C; δ_H 1.65–1.85 (m, 6 H), 1.94 (bs, 2 H), 2.23 (bs, 3 H), 2.38 (s, 3 H), 2.45–2.55 (m, 2 H), 3.15 (s, 2 H), 7.15–7.25 (m, 2 H), 7.50–7.60 (m, 2 H); δ_C 21.42 (C_{CH₃}), 29.82 (C₇, J = 9.7 Hz), 33.96 (C_{8,10}, J = 1.6 Hz), 38.27 (C_{4,9}, J = 19.0 Hz), 39.88 (C_{1,3}, J = 10.3 Hz), 42.38 (C₆, J = 17.7 Hz), 43.17 (C_{4'}, J = 1.6 Hz), 88.93 (C₂, J = 1.6 Hz), 91.00 (C₅, J = 184.5 Hz), 126.31 (C₀), 127.15 (C_i), 129.37 (C_m),

140.15 (C_p), 155.99 (C₃); MS (EI, m/z) 299 (M⁺, 100), 282 (34), 158 (12), 131 (23), 91 (29); HRMS calcd for C₁₉H₂₂NOF 299.1687, found 299.1678. Anal. Calcd for C₁₉H₂₂NOF: C, 76.22; H, 7.41; N, 4.68.

E-8-F,Me: colorless solid; mp 165–166.5 °C; δ_H 1.52 (bs, 1 H), 1.56 (bs, 1 H), 1.96 (bs, 6 H), 2.15–2.35 (m, 5 H), 2.38 (s, 3 H), 3.20 (s, 2 H), 7.15–7.25 (m, 2 H), 7.50–7.60 (m, 2 H); δ_C 21.43 (C_{CH₃}), 29.41 (C₇, J = 9.9 Hz), 31.71 (C_{8,10}, J = 2.0 Hz), 39.30 (C_{1,3}, J = 10.1 Hz), 40.06 (C_{4,9}, J = 18.9 Hz), 42.43 (C₆, J = 16.8 Hz), 44.24 (C_{4'}), 89.27 (C₂), 91.12 (C₅, J = 184.6 Hz), 126.31 (C₀), 127.64 (C_i), 129.38 (C_m), 140.18 (C_p), 156.16 (C₃); MS (EI, m/z) 299 (M⁺, 100), 282 (25), 269 (9), 158 (11), 131 (20), 91 (26); HRMS calcd for C₁₉H₂₂NOF 299.1687, found 299.1685. Anal. Calcd for C₁₉H₂₂NOF: C, 76.22; H, 7.41; N, 4.68, found C, 76.10; H, 7.46; N, 4.70.

General Procedure for the Synthesis of 5-Substituted-3'-phenyladamantane-2-spiro-5'-(Δ²-1',2',4'-oxadiazolines) E and Z-11-X,H. *E*- and *Z*-11-X,H were synthesized by a procedure similar to that of Ito^{9b,c} and Westheimer et al.^{13,14} About 0.5 g of molecular sieves are added to a solution of 0.2 g of ketone 1-X and benzylamine (1.5 mol equiv of ketone) in 10 mL of benzene. The mixture was stirred at reflux for 15 h, and the molecular sieve was removed and washed with solvent. After solvent evaporation, the solid residue 4-X was added to benzohydroximoyl chloride 6-H (1.5 mol equiv of ketone) in 10 mL of dry dichloromethane. Excess of triethylamine (1.5 mol equiv) was added to the mixture. The mixture was stirred at room temperature for 0.5 h, washed with water, and then dried with MgSO₄. After filtration and solvent evaporation, the residue was purified on a silica gel column by *n*-hexane/methylene chloride to give two isomeric adducts *E*- and *Z*-11-X,H. Recrystallization from *n*-hexane/methylene chloride at room temperature gave white needle crystalline *Z*-11-H,H. All the *E*-11-X,H adduct except *E*-11-F,H could not be isolated by liquid chromatography and recrystallization. The ¹³C NMR spectra can be obtained, however, from *E*- and *Z*-11-X,H mixtures. The isolated yields based on converted starting materials 1-X are as follows: **11-F,H** 83%, **11-Cl,H** 87%, **11-Br,H** 86%, **11-Ph,H** 92%.

11-H,H: colorless solid, mp 205–207 °C; δ_H 1.55–1.80 (m, 6 H), 1.80–1.95 (m, 2 H), 2.00–2.15 (m, 2 H), 2.15–2.35 (m, 4 H), 4.48 (s, 2 H), 7.10–7.45 (m, 8 H), 7.55–7.68 (m, 2 H); δ_C 26.67 (C₇), 26.88 (C₅), 34.56 (C_{8,10}), 34.43 (C_{1,3}), 34.73 (C_{4,9}), 37.35 (C₆), 49.73 (C₁₁), 102.42 (C₂), 126.80 (d), 126.96 (s), 127.01 (d), 128.34 (d), 128.41 (d), 128.56 (d), 130.45 (d), 139.67 (s), 161.28 (C₃); MS (EI) m/z 359 (M⁺ + 1, 6), 358 (M⁺, 22), 238 (4), 237 (4), 193 (21), 150 (16), 121 (54), 91 (100), 79 (80); HRMS calcd for C₂₄H₂₆ON₂: C, 80.41; H, 7.31, found: C, 80.35; H, 7.30.

Z-11-F,H: colorless solid; mp 153.5–155 °C; δ_H 1.55–1.80 (m, 4 H), 1.85–2.05 (m, 4 H), 2.10–2.20 (m, 1 H), 2.35–2.55 (m, 4 H), 4.47 (s, 2 H), 7.10–7.27 (m, 5 H), 7.27–7.45 (m, 3 H), 7.55–7.70 (m, 2 H); δ_C 29.67 (C₇, J = 9.9 Hz), 32.39 (C_{8,10}, J = 2.0 Hz), 36.93 (C_{1,3}, J = 10.6 Hz), 39.18 (C_{4,9}, J = 19.5 Hz), 42.36 (C₆, J = 17.6 Hz), 49.90 (C₁₁), 90.94 (C₅, J = 184.3 Hz), 100.61 (C₂), 126.36 (s), 126.64 (d), 127.27 (d), 128.32 (d), 128.57 (d), 128.71 (d), 130.74 (d), 139.14 (s), 161.37 (C₃); MS (EI) m/z 376 (M⁺, 48), 255 (10), 235 (7), 193 (4), 168 (5), 105 (58), 91 (100), 77 (9); HRMS calcd for C₂₄H₂₅ON₂F: C, 76.57; H, 6.69; N, 7.44, found C, 76.62; H, 6.63; N, 7.49.

E-11-F,H: colorless solid; mp 132–132.5 °C; δ_H 1.47 (bs, 1 H), 1.51 (bs, 1 H), 1.77 (bs, 1 H), 1.78 (bs, 1 H), 1.79–1.95 (m, 2 H), 2.10–2.35 (m, 5 H), 2.39 (bs, 2 H), 4.50 (s, 2 H), 7.15–7.30 (m, 5 H), 7.30–7.45 (m, 3 H), 7.60–7.68 (m, 2 H); δ_C 29.61 (C₇, J = 9.9 Hz), 33.12 (C_{8,10}, J = 1.9 Hz), 36.94 (C_{1,3}, J = 10.2 Hz), 38.67 (C_{4,9}, J = 19.4 Hz), 42.44 (C₆, J = 16.8 Hz), 49.79 (C₁₁), 91.32 (C₅, J = 184.4 Hz), 100.64 (C₂), 126.40 (s), 126.66 (d), 127.31 (d), 128.33 (d), 128.60 (d), 128.73 (d), 130.76 (d), 139.16 (s), 161.36 (C₃); MS (EI) m/z 376 (M⁺, 57), 255 (13), 235 (11), 193 (5), 168 (7), 105 (68), 91 (100), 77 (10); HRMS calcd for C₂₄H₂₅ON₂F 376.1952, found 376.1944.

Z-11-Cl,H: colorless solid; mp: 182–183.5 °C; δ_H 1.67 (bd, J = 12.8 Hz, 2 H), 1.90–2.10 (m, 4 H), 2.10–2.25 (m, 3 H), 2.35 (bs, 2 H), 2.71 (bd, J = 12.3 Hz, 2 H), 4.46 (s, 2 H), 7.15–

7.30 (m, 5 H), 7.30–7.50 (m, 3 H), 7.60–7.70 (m, 2 H); δ_{C} 29.89 (C₇), 32.13 (C_{8, 10}), 37.26 (C_{1,3}), 44.14 (C_{4,9}), 47.29 (C₆), 49.88 (C₁₁), 65.95 (C₅), 100.40 (C₂), 126.38 (s), 126.65 (d), 127.30 (d), 128.36 (d), 128.60 (d), 128.73 (d), 130.78 (d), 139.17 (s), 161.39 (C₃); MS (EI) *m/z* 394 (M⁺ + 2, 8), 392 (M⁺, 22), 357 (M⁺ – ³⁵Cl, 1), 266 (6), 105 (48), 91 (100), 77(13); HRMS calcd for C₂₄H₂₅ON³⁵Cl 392.1658, found 392.1663. Anal. Calcd for C₂₄H₂₅ONCl: C, 73.36; H, 6.41; N, 7.13, found C, 73.23; H, 6.42; N, 7.25.

E-11-Cl,H: δ_{C} 30.21 (C₇), 32.49 (C_{8, 10}), 36.91 (C_{1,3}), 43.40 (C_{4,9}), 47.08 (C₆), 49.53 (C₁₁), 65.95 (C₅), 100.02 (C₂), 161.05 (C₃).

Z-11-Br,H: colorless solid; mp: 186–187 °C; δ_{H} 1.65–1.80 (m, 2 H), 2.00–2.25 (m, 5 H), 2.25–2.40 (m, 4 H), 2.85–3.00 (m, 2 H), 4.45 (s, 2 H), 7.15–7.30 (m, 5 H), 7.30–7.45 (m, 3 H), 7.60–7.70 (m, 2 H); δ_{C} 30.69 (C₇), 32.10 (C_{8, 10}), 38.10 (C_{1,3}), 45.65 (C_{4,9}), 48.81 (C₆), 49.83 (C₁₁), 62.47 (C₅), 100.30 (C₂), 126.38 (s), 126.65 (d), 127.31 (d), 128.35 (d), 128.60 (d), 128.73 (d), 130.77 (d), 139.14 (s), 161.38 (C₃); MS (EI) *m/z* 438 (M⁺ + 2, 14), 436 (M⁺, 14), 357 (M⁺ – ⁷⁹Br, 4), 266 (16), 236 (15), 149 (16), 105 (49), 91 (100), 77(17); HRMS calcd for C₂₄H₂₅ON⁷⁹Br 436.1152, found 436.1155. Anal. Calcd for C₂₄H₂₅ONBr: C, 65.91; H, 5.76; N, 6.40, found C, 65.94; H, 5.77; N, 6.58.

E-11-Br,H: δ_{C} 30.61 (C₇), 32.67 (C_{8, 10}), 38.00 (C_{1,3}), 45.11 (C_{4,9}), 48.70 (C₆), 49.75 (C₁₁), 62.68 (C₅), 100.11 (C₂), 161.30 (C₃).

Z-11-Ph,H: colorless solid; mp: 114.5–116 °C; δ_{H} 1.65–1.80 (m, 4 H), 1.94 (bs, 2 H), 2.05–2.20 (m, 3 H), 2.30–2.40 (m, 2 H), 2.45–2.60 (m, 2 H), 4.53 (s, 2 H), 7.10–7.45 (13 H), 7.60–7.70 (m, 2 H); δ_{C} 27.43 (C₇), 32.16 (C_{8, 10}), 34.86 (C_{1,3}), 35.14 (C₅), 40.29 (C_{4,9}), 42.49 (C₆), 49.85 (C₁₁), 101.76 (C₂), 124.93 (d), 125.72 (s), 126.76 (d), 127.10 (d), 128.11 (d), 128.34 (d), 128.47 (d), 128.62 (d), 130.56 (d), 139.52 (s), 149.60 (s),

161.38 (C₃); MS (EI) *m/z* 434 (M⁺, 57), 314 (11), 266 (19), 155 (28), 105 (48), 91 (100), 77 (14); HRMS calcd for C₃₀H₃₀ON₂ 434.2360, found, 434.2368. Anal. Calcd for C₃₀H₃₀ON₂: C, 82.91; H, 6.96; N, 6.45, found C, 83.03; H, 6.99; N, 6.56.

E-11-Ph,H: δ_{C} 26.99 (C₇), 33.51 (C_{8, 10}), 34.57 (C_{1,3}), 35.02 (C₅), 39.20 (C_{4,9}), 42.42 (C₆), 49.37 (C₁₁), 101.58 (C₂), 161.09 (C₃).

Computational Methods. The AM1¹⁵ method was employed to calculate all the reactants of the 1,3-dipolar cycloaddition reactions including dipolarophiles (**1-X** to **4-X**) and benzonitrile oxide **5-Y**. The reactants were fully optimized without any constraint. Frequency calculations were carried out for every optimized structures. All the reactants are located in the local minimum on the potential energy surface confirmed by all real-frequencies. The calculations were performed with the SPARTAN 5.0 program.¹⁶

Acknowledgment. This work is supported at NCTU by the National Science Council of the Republic of China (Grant NSC-87-2113-M-009-002).

Supporting Information Available: AM1-calculated energies for frontier molecular orbitals of **2**- to **5-X**, ¹H and ¹³C NMR spectra for compounds **E-7-F,Y** (Y = Cl, Br), **Z-7-F,Y** (Y = F, Cl, Br, NO₂ and Me), **Z-8-F,Cl** and **Z-** and **E-8-F,X** (X = CN, NO₂ and OMe), and **E-11-F,H**; X-ray crystallography data for **Z-7-Br,H**. This material is available free of charge via the Internet at <http://pubs.acs.org>.

JO980945N

(16) Spartan version 5.0, USA: Wavefunction, Inc., 1998. We thank the National Center for High-performance Computing for support of the calculation.